Biogeosciences Discuss., doi:10.5194/bg-2016-380, 2016
Manuscript under review for journal Biogeosciences
Published: 15 September 2016

Biogeosciences Discussions Open Access EGU

Influence urban infrastructure on water quality and greenhouse gas dynamics in streams

Rose M. Smith[1,2], Sujay S. Kaushal[2], Jake J. Beaulieu[3], Michael J. Pennino[4,5], Claire Welty[5]

[1] Department of Biology, University of Utah, Salt Lake City, UT, 84112, USA
[2] Department of Geology, University of Maryland, College Park, MD, 20742, USA
[3] U.S. Environmental Protection Agency, Office of Research and Development, National Risk Management Research Laboratory, Cincinnati, OH, 45220, USA
[4] U.S. Environmental Protection Agency National Health and Environmental Effects Research Lab, Corvallis, OR, 97333, USA
[5] Department of Chemical, Biochemical, and Environmental Engineering and Center for Urban Environmental Research and Education, University of Maryland Baltimore County, Catonsville, MD, 21250, USA

Correspondence to: Rose M. Smith[1] (rose.smith@utah.edu)

Abstract. Streams and rivers are significant sources of nitrous oxide (N_2O), carbon dioxide (CO_2), and methane (CH_4), and watershed management can alter greenhouse gas (GHG) emissions from streams. GHG emissions from streams in agricultural watersheds have been investigated in numerous studies, but less is known about streams draining urban watersheds. We hypothesized that urban infrastructure significantly influences GHG dynamics along the urban watershed continuum, extending from engineered headwater flowpaths to larger streams. GHG concentrations and emissions were measured across streams draining a gradient of stormwater and sanitary infrastructure including: 1) complete stream burial, 2) in-line stormwater wetlands, 3) riparian/ floodplain preservation, and 4) septic systems. Infrastructure categories significantly influenced drivers of GHG dynamics including carbon to nitrogen stoichiometry, dissolved oxygen, total dissolved nitrogen (TDN), and water temperature. These variables explained much of the statistical variation in nitrous oxide (N_2O), carbon dioxide (CO_2), and methane (CH_4) saturation in stream water (r^2 = 0.78, 0.78, 0.50 respectively). N_2O saturation ratios in urban streams were among the highest reported for flowing waters, ranging from 1.1 - 47 across all sites and dates. The highest N_2O saturation ratios were measured in streams draining nonpoint N sources from septic systems and were strongly correlated with TDN. CO_2 was highly correlated with N_2O across all sites and dates (r^2=0.84), and CO_2 saturation ratio ranged from 1.1 - 73. CH_4 was always super-saturated with saturation values ranging from 3.0 to 2,157. Differences in stormwater and sewer infrastructure influenced water quality, with significant implications for enhancing or minimizing stream CO_2, CH_4, and N_2O emissions.

Key Words: Greenhouse Gases, Urban Streams, Infrasturcutre, DOC, nitrate, methane, carbon dioxide, methane, nitrous oxide

Biogeosciences Discuss., doi:10.5194/bg-2016-380, 2016
Manuscript under review for journal Biogeosciences
Published: 15 September 2016

1 Introduction

Streams and rivers are globally significant sources of nitrous oxide (N_2O), carbon dioxide (CO_2), and methane (CH_4) (e.g., Seitzinger et al. 2000; Beaulieu et al. 2011; Bastviken et al. 2011; Raymond et al. 2013). The interactive effects of climate and land cover change have increased greenhouse gas emissions (GHG) from streams and rivers by altering the biogeochemical controls of ecosystem metabolism (i.e., nutrient stoichiometry, organic matter quality, redox state, and temperature), (e.g. Kaushal et al. 2014a; Beaulieu et al. 2009; Dinsmore et al. 2009; Baulch et al. 2011; Harrison and Matson 2003). Urban stormwater and sanitary sewer infrastructure – including stormwater wetlands, stream burial in pipes, gravity sanitary sewer lines, and septic systems – influences nutrient loading (Shields et al. 2008; Kaushal and Belt 2012; Newcomer et al. 2012; Pennino et al. 2014; Beaulieu et al. 2015) and may have implications for GHG production as well. Numerous studies have examined the role of point sources of nutrients such as wastewater treatment plant (WWTP) effluent on urban N_2O emissions (Foley et al. 2010; Townsend-Small et al. 2011; Strokal and Kroeze 2014; Beaulieu et al. 2010), but few have examined the role of nonpoint source nutrient loading on N_2O emissions from urban streams. The nonpoint source N loads from gravity sewers and septic systems, however, may contribute substantially to urban N_2O emissions (Beaulieu et al. 2010; Short et al. 2014). Aquatic N_2O production and emissions have been linked to microbial transformations of excess N loading, as well as reduced oxygen availability (Beaulieu et al. 2011; Rosamond et al. 2012). While stormwater-control wetlands and other forms of green infrastructure (GI) may reduce N_2O production in streams by reducing excess N inputs, GI may increase both N_2O and CH_4 inputs to streams and groundwater due to CH_4 and N_2O production that occurs within the GI unit (Søvik et al. 2006; VanderZaag et al. 2010). Despite considerable funds spent on restoring aging infrastructure and improving water quality in cities globally (Doyle et al. 2008), the role of urban water infrastructure on biogeochemical cycles and GHG production is a major source of uncertainty.

The International Panel on Climate Change (IPCC) includes N_2O emissions from agricultural, but not urban streams, in the global N_2O inventory based on nitrogen inputs from fertilizer and manure (Nevison 2000; Ciais et al. 2013; UNEP 2013; Strokal and Kroeze 2014; Short et al. 2014). N loading to streams can be as high in urban as in agricultural watersheds, but the relationship between N and N_2O emissions may differ substantially in urban and agricultural watersheds. Some key differences include: 1) the source and quantity of anthropogenic N loading to streams, 2) the C:N ratio of stream water and groundwater, and 3) the degree to which surface and groundwater flowpaths are altered by infrastructure. These factors are likely to be influenced by stormwater and sanitary sewer infrastructure designs (Søvik et al. 2006; Collins et al. 2010; Kaushal et al. 2011). Stormwater management may promote anoxic conditions and increase C:N ratio of stream water if wetlands are created along the urban watershed continuum (e.g. Søvik et al. 2006; Newcomer et al. 2012). Stormwater management can reduce C:N ratios, if streams are buried in storm drains (Elmore and Kaushal 2008; Pennino et al. 2016; Beaulieu et al. 2014). Sanitary sewer infrastructure may additionally contribute to GHG emissions from urban streams by direct leakage of gases or excess nitrogen from sewer lines (Yu et al. 2013; Short et al. 2014).

Biogeosciences Discuss., doi:10.5194/bg-2016-380, 2016
Manuscript under review for journal Biogeosciences
Published: 15 September 2016

Inverse relationships between dissolved organic carbon (DOC) and nitrate (NO_3^-) concentrations persist across a wide variety of ecosystems ranging from soils to streams to oceans (e.g., Aitkenhead-Peterson and McDowell 2000; Dodds et al. 2004; Kaushal and Lewis 2005; Taylor and Townsend 2010). Recently, inverse relationships between DOC and NO_3^- have also been reported for urban environments from groundwater to streams to river networks (Mayer et al. 2010; Kaushal and Belt 2012; Kaushal et al. 2014a). A suite of competing biotic process may control this relationship, by either: 1) assimilating or reducing NO_3^- in the presence of bioavailable DOC, or 2) producing NO_3^- regardless of DOC status (Hedin et al. 1998; Dodds et al. 2004; Kaushal and Lewis 2005; Taylor and Townsend 2010). The former category includes heterotrophic denitrification, which oxidizes organic carbon to CO_2 and reduces NO_3^- to $N_2O + N_2$ (Knowles, 1982), and assimilation of inorganic N (Wymore et al. 2015; Caraco et al. 1998; Kaushal and Lewis 2005). In the second category, nitrification is a chemoautotrophic process that produces NO_3^- by oxidizing NH_4^+, and consumes CO_2. Nitrification also yields N_2O as an intermediate product, and has been shown to dominate N cycling processes in low-DOC environments (Taylor and Townsend, 2010). In urban watersheds, denitrification is often limited by DOC due to increased N loading and/or decreased connectivity with carbon-rich soils in the riparian zone (Mayer et al. 2010; Newcomer et al. 2012). The interactive effects of increased anthropogenic C and N loading and biogeochemical transformations have the potential to alter GHG production and emissions from streams (Kaushal et al. 2014b).

The goal of the present study was to identify patterns and potential drivers related to GHG dynamics in urban headwater streams draining different forms of infrastructure (stream burial, septic systems, in-line SWM wetlands and riparian/floodplain preservation). Although less considered, GHG emissions may be an unintended consequence of urban water quality impairments and biogeochemical processes occurring within and downstream of urban infrastructure. An improved understanding of the relationship between infrastructure type and biogeochemical functions along the urban watershed continuum is critical for minimizing unintended consequences of water quality management (Kaushal and Belt 2012). Additionally, a better understanding of the contribution of urban watersheds to global GHG emissions will be critical, given that urbanization is the fastest form of land-use change and urban areas contain greater than 60% of Earth's population (Foley et al. 2005; Bellucci et al. 2012; Ciais et al. 2013).

2.1 Sampling Methods

2.1.1 Study Sites

Eight headwater streams that are part of the Baltimore Long-Term Ecological Research (LTER) project (www.beslter.org) were sampled every two weeks for water chemistry and dissolved gases. Sampling sites were located in the Red Run and Dead Run subwatersheds of the Gwynns Falls that were developed at different times (Fig. 1). Previous work in the Baltimore LTER project has extensively characterized the hydrology, biogeochemistry, and geomorphology of the Gwynns Falls stream network (*e.g.*, Doheny 1999; Groffman et al. 2004, Nelson et al. 2006; Kaushal et al. 2008, Shields et al. 2008, Meierdiercks et al. 2010;

Biogeosciences Discuss., doi:10.5194/bg-2016-380, 2016
Manuscript under review for journal Biogeosciences
Published: 15 September 2016

Ryan et al. 2010; Sivirichi et al. 2011, Newcomer et al. 2012; Newcomer Johnson et al. 2014; Pennino et al. 2014; Pennino et al. 2016; Bhaskar et al. 2012, 2015).

Study sites were selected based on differences in stormwater and sanitary sewer infrastructure within each of eight headwater watersheds. Dead Run (15 km^2) and Red Run (17 km^2) are both dominated by medium to high-density residential and commercial land. Dead Run was developed between the 1950s and 1970s, with channelized or buried streams as part of the stormwater infrastructure and aging sanitary sewer lines that are often cracked and leaking to the subsurface. Stormwater wetlands and ponds drain a portion of the Dead Run watershed and are located in-line with stream channels. In contrast, Red Run was intensively developed in the 2000s and stormwater infrastructure reflects more infiltration-based designs such as stream buffer zones, infiltration wetlands, and bio-retention cells throughout the landscape (Baltimore County Department of Planning, 2010). Sanitary sewers were constructed in this watershed between 2000 and 2010 (Baltimore County Department of Planning, 2000). A few small areas with low-density development built in the 1960s that are served by septic systems are located in the northern part of Red Run (Fig. 1).

The eight study streams drained various forms of stormwater and sanitary infrastructure. We define stormwater infrastructure broadly to encompass older designs such as stormwater drainage networks, which are designed to convey stormwater away from the landscape rapidly and often incorporate buried streams at downgradient locations since the large collector pipes are installed at low points in the landscape, coincident with stream valleys and exhibit perennial flow. Newer forms of 'green' stormwater infrastructure (GI) include infiltration wetlands and stream channel/ floodplain modifications, which are designed to attenuate peak runoff during storms. Sanitary infrastructure exists in varying forms (gravity sewers and septic systems) as well as a gradient of sewer line ages, which can often be inferred from housing age, assuming no major sewer line replacement has occurred. We selected eight headwater stream watersheds, each of which drained one of four distinct infrastructure typologies. These typologies were based on having similar land cover, development age, stormwater infrastructure design, and sanitary infrastructure. A comprehensive description of attributes in each typology can be found in Table 1, however for simplicity we have abbreviated the typologies based on the dominant infrastructure feature as follows: 1) stream burial, 2) in-line stormwater management (SWM) wetlands, 3) riparian/floodplain preservation, and 4) septic systems.

2.1.2 Temporal Sampling of Dissolved Gases and Stream Chemistry

Dissolved gas samples were collected every other week from eight headwater sites (first order streams) draining the typologies described above and in Table 1 ('Stream Burial,' 'In-Line SWM Wetlands', 'Riparian/Floodplain Preservation' and 'Septic Systems'). Five replicate samples were collected per stream on each date. Samples were collected by submerging a 140 mL syringe with a 3-way luer-lock and pulling 115 mL of stream water into the syringe. Next, 25 mL of ultra-high purity helium was added to the syringe, which was then shaken for 5 minutes to promote the equilibration of gases between the aqueous and gas phase. After equilibration, 20 mL of the headspace was transferred into a pre-evacuated glass vial capped with screw-top rubber septa (LabCo Limited, Lampeter, UK) and stored at room temperature for up to four weeks prior to analyses. Water

Biogeosciences Discuss., doi:10.5194/bg-2016-380, 2016
Manuscript under review for journal Biogeosciences
Published: 15 September 2016

temperature and barometric pressure during the equilibration were recorded and three blank samples were taken at each field site.

Stream water samples were collected in 250 mL high-density polyethylene bottles at each site. Single samples were taken at each site, with one rotating site duplicated on each sampling date. Dissolved oxygen (DO) concentration and pH were measured at the upstream end of each study reach using a handheld YSI 550-A dissolved oxygen meter (YSI Inc. Yellow Springs, OH) and an Oakton handheld pH meter (Oakton Instruments, Vernon Hills, IL).

2.1.3 Longitudinal Sampling of Dissolved Gases along the Urban Watershed Continuum

Longitudinal surveys were conducted in June 2012, March 2014, and December 2014 along the two main paired watersheds of Red Run and Dead Run. Longitudinal sampling started at the confluence with each major tributary (Dead Run or Red Run) and Gwynns Falls, and extended every 500 m to upstream toward biweekly sampled headwater sites (Fig. 1). During spring and fall months, solute and gas samples were collected along all major tributaries (>5% main stem flow) as well as every 500 m along the main stem of Dead Run and Red Run. Stream discharge was measured at each sampling point using a Marsh-McBirney Flo-Mate hand held velocity meter (Marsh McBirney Inc., Frederick, MD, USA). Discharge measurements were made by taking cross-sectional measurements of stream velocity and water depth at each site. A minimum of 10 points was measured along each cross section. Where sampling points were co-located with USGS gaging stations, discharge data was provided by USGS.

Locations for each sampling site were either recorded with a handheld GPS or estimated using Google Earth software. The watershed contributing area above each sampling point and flow length from each sampling point to the watershed outlet (Dead Run or Red Run respectively) were calculated using ArcMap 10 using a 1-meter LiDAR digital elevation model of the Gwynns Falls watershed obtained from Baltimore County (http://imap.maryland.gov/Pages/lidar.aspx). These surveys were used to determine whether or not the patterns in GHGs and solute concentrations within headwater streams were present along the broader urban watershed continuum encompassing engineered flowpaths from headwaters to higher order streams. Reach-scale hydrologic mass balances were calculated along the main stem of Red Run and Dead Run from these synoptic surveys following methods detailed previously (Kaushal et al. 2014a, Newcomer Johnson et al. 2014). Along each reach of the main stem, relative contributions of inflow were calculated following Eq. (1):

$$Q_{GW} = Q_{DS} - Q_{US} - Q_{TRIB,} \quad (1)$$

where Q_{GW} is the net groundwater input, estimated by difference using field measurements of Q_{DS}, Q_{US}, and $Q_{TRIB.}$ Q_{DS} is discharge measured in the main stem (m^3 s^{-1}) at the bottom of a reach, Q_{US} is discharge in the main stem at the top of a reach, Q_{TRIB} is inflow from major tributaries.

Biogeosciences Discuss., doi:10.5194/bg-2016-380, 2016
Manuscript under review for journal Biogeosciences
Published: 15 September 2016

2.2 Laboratory Methods

2.2.1 Dissolved Gas Concentrations

Samples of headspace equilibrated gas concentrations (CO_2, CH_4, and N_2O) were stored at room temperature for up to 1 month in airtight exetainer vials and transported to the EPA National Risk Management Research Laboratory, Cincinnati, Ohio for analysis. Concentrations of CO_2, CH_4, and N_2O were measured using a Bruker 450 (Billerica, MA, U.S.A) gas chromatograph equipped with a methanizer, flame ionization detector (FID), and electron capture detector (ECD). Instrument detection limits were 100 ppb for N_2O, 10 ppm for CO_2, and 0.1 ppm for CH_4.

2.1.2 Solute Concentrations

Water samples were transported on ice to University of Maryland and filtered using pre-combusted 0.7 µm glass fiber filters within 24 hours. A Shimadzu analyzer (Shimadzu Scientific, Kyoto Japan) was used to measure total dissolved nitrogen (TDN) and dissolved organic carbon (DOC). The non-purgeable organic carbon (NPOC) method was utilized for DOC, despite potential under-estimates of volatile compounds because it is insensitive to variations in DIC (Findlay et al. 2010). Nitrate (NO_3^-) concentrations were measured *via* colorimetric reaction using a cadmium reduction column (Lachat method 10-107-04-1-A) on a Lachat flow injection analyzer (Hach, Loveland, CO).

2.1.3 Dissolved Organic Matter Characterization

Filtered water samples were analyzed for optical properties in order to characterize dissolved organic matter sources. Filtered water samples were stored in amber glass vials at 4ºC for a maximum of two weeks prior to analyses. Detailed methodology for optical properties and fluorescence indices can be found in Smith and Kaushal (2015). Briefly, fluorescence and absorbance properties of dissolved organic matter (DOM) were measured in order to evaluate the relative abundance of terrestrial (high molecular weight plant/soil –derived humic acids) and aquatic (low molecular weight bacterial or planktonic compounds) sources to the overall dissolved organic matter pool.

A FluoroMax-4 Spectrofluorometer (Horiba Jobin Yvon, Edison NJ, USA) was used to measure the emission spectra of samples in response to a variety of excitation wavelengths. Excitation-emission matrices (EEMs) were used for characterizing indices of terrestrial *vs.* aquatic DOM sources. For example, the humification index (also known as HIX) is defined as the ratio of emission intensity of the 435-480 nm region of the EEM to the emission intensity of the 300-345 nm region of the EEM at the excitation wavelength of 254 nm (Zsolnay et al. 1999; Ohno 2002). The humification index varies from 0 to 1, with higher values signifying high-molecular weight DOM molecules characteristic of humic terrestrial sources. Lower humification index values indicate low molecular weight DOM of bacterial or aquatic origin (Zsolnay et al. 1999). The autochthonous inputs index (also known as BIX) is defined as the ratio of fluorescence intensity at the emission wavelength 380 nm to the intensity emitted at 430 nm at the excitation wavelength of 310 nm (Huguet et al. 2009). Lower autochthonous

Biogeosciences Discuss., doi:10.5194/bg-2016-380, 2016
Manuscript under review for journal Biogeosciences
Published: 15 September 2016

inputs index values (<0.7) represent terrestrial sources, and higher autochthonous inputs index values (>0.8) represent algal or bacterial sources (Huguet et al. 2009).

2.3 Calculations

Dissolved gas concentrations were calculated using Eq.'s (2- 4). First, we used Henry's law to convert measured mixing rations (ppmv) to the molar concentration of each gas in the headspace vial [C_g], (µmol L^{-1}) following Eq. (2),

$$[C] = \frac{PV}{RT}, \quad (2)$$

where P is pressure (1 atm), V is the measured partial pressure of the gas of interest (ppmv), R is the universal gas constant (0.0821 L atm mol^{-1} K^{-1}), and T is the temperature of a water sample during headspace equilibration (K).

We used Henry's law and a temperature-corrected Bunsen solubility coefficient to calculate [C_{aq}], the concentration of residual gas remaining in water following headspace equilibration (Eq. 3) (Stumm and Morgan 1981)

$$[C_{aq}] = \frac{V*Bp*Bunsen}{RT}, \quad (3)$$

where V is measured gas mixing ratio (ppmv), Bp is the barometric pressure (atm), and Bunsen is the solubility coefficient in the vessel (L L^{-1} atm^{-1}). Calculations of the Bunsen coefficient were based on Weiss (1974) for CO_2, Weiss (1970) for N_2O, and Yamamoto et al., (1976) for CH_4.

The final stream water concentration [C_{str}] was then calculated using mass balance of these two pools, described in Eq. (4), where V_{aq} and V_g were the volumes of water and gas respectively in a water sample with helium headspace.

$$[C_{str}] = \frac{[C_{aq}]*V_{aq}+[C_g]*V_g}{RT}, \quad (4)$$

Because gas solubility is temperature-dependent, it was useful to display gas concentrations as the percent saturation, or the ratio of the measured dissolved gas concentration to the equilibrium concentration. To determine gas saturation, the equilibrium concentration ([C_{eq}]) was calculated based on water temperature, atmospheric pressure, and an assumed value for the current atmospheric mixing ratios of each gas following Eq. (3) (CO_2: https://scripps.ucsd.edu/programs/keelingcurve/, N_2O: www.esrl.noaa.gov/gmd/hats/combined/N2O.html, CH_4: www.esrl.noaa.gov/gmd/ccgg/trends_ch4/). Saturation ratio is defined as a ratio [C_{str}] / [C_{eq}], while excess (i.e *xs*CO_2) is described as a mass difference ([C_{str}] - [C_{eq}]).

2.3.2 Index of aerobic and anaerobic respiration

Comparing the gas saturation ratio of different gases can provide evidence of the biogeochemical processes responsible for the production or consumption of biogenic gases. However, the biological influence on dissolved gas concentration can be confounded with the physical effects of gas exchange. To correct for the effect of different gas exchange rates across streams,

Biogeosciences Discuss., doi:10.5194/bg-2016-380, 2016
Manuscript under review for journal Biogeosciences
Published: 15 September 2016

we calculated the ratios between apparent oxygen utilization (AOU) and *xs*CO_2. AOU is calculated as the difference between O_2 concentration at equilibrium with the atmosphere and measured dissolved oxygen in the stream. Positive values of AOU therefore signify net consumption of O_2 along watershed flowpaths, and negative AOU values signify net production O_2. Under aerobic conditions, respiration of organic matter consumes O_2 and produces CO_2 in approximately a 1:1 molar ratio (Schlessinger 1997). Therefore, 1 mole of AOU should result in 1 mol of *xs*CO_2. This ratio was then used, with an offset to 1.2:1 to account for differences in diffusion constants for the two gases (Stumm and Morgan 1981; Richey et al. 1988), to determine the proportion of CO_2 produced from aerobic respiration. For instance, 1 mol of AOU would result in 1 mol of CO_2 excess if aerobic respiration where the only CO_2 source. A CO_2 excess value greater than 1 mol would be indicative of other CO_2 sources, namely anaerobic respiration, which produces CO_2 without consuming O_2. This framework was used to calculate the percentage of CO_2 produced from anaerobic *vs.* abiotic processes. Anaerobic CO_2 concentrations were calculated as the difference between aerobically produced CO_2 (assumed equivalent to AOU) and measured CO_2 concentration.

2.3.3 Greenhouse gas emissions

Gas emissions were calculated using Eq. (5), in which, and F_{GHG} is the flux (g m^{-2} d^{-1}) of a given gas at ambient temperature, d is water depth (m), and K_{GT} (day^{-1}), is the air-water gas exchange rate for a given gas at ambient temperature as in Eq. (4)

$$F_{GHG} = K_{GT} * \mathrm{d} * \left([C_{str}] - [C_{eq}]\right), \quad (5)$$

The air-water gas exchange rate was estimated for each site and sampling date using an energy dissipation model (Tsivoglou and Neal 1976). This model describes K_{20} as a function of water velocity (V, m day^{-1}), water surface gradient (S), and a site-specific constant called the escape coefficient ($C_{esc,}$ m^{-1}) (Eq. 6).

$$K_{20} = C_{esc} * \mathrm{S} * \mathrm{V}, \quad (6)$$

We estimated S at each GHG sampling site by measuring the change in elevation over a reach with a handheld GPS unit. We estimated S for reaches in Pennino et al (2014) using digital elevation data from Google Earth at the top and bottom of each known sampling reach. C_{esc} is a parameter related to additional factors other than streambed slope and velocity that affect gas-exchange including streambed roughness and the relative abundance of pools and riffles. We estimated C_{esc} for our sampling sites using measurements of sulfur hexafluoride (SF_6) gas exchange rate (K_{SF6}) from 15 tracer injection experiments carried out across a range of flow conditions in four streams within 5 km^2 of our study sites (Pennino et al. 2014).

C_{esc} was calculated to be 0.198 m^{-1} (n=15, r^2=0.81, P= 5.48 x10 $^{-6}$). The 95% confidence interval of this C_{esc} based on measured K_{20} values was ±0.058 which corresponds to ±29% of a given gas flux estimate. This estimate of C_{esc} from these nearby sites was assumed to be representative of the 8 stream reaches investigated in this study. The uncertainty associated with C_{esc} was small compared to the difference in estimated flux across sites. Areal flux data was thus interpreted with caution, and only examined in terms of the magnitude across all sites and in comparisons with literature values.

Biogeosciences Discuss., doi:10.5194/bg-2016-380, 2016
Manuscript under review for journal Biogeosciences
Published: 15 September 2016

We converted K_{SF6} to K for CO_2, CH_4, and N_2O by multiplying K_{SF6} by the ratio of Schmidt numbers for SF_6 and each measured gas (Stumm and Morgan 1981). K was also adjusted to 20°C (K_{20}) following Eq. (7), where K_T is K for a given gas at ambient temperature

$$K_{20} = \frac{K_T}{1.0421^{T-20}}, \quad (7)$$

2.4 Statistical Analyses

2.4.1 Role of infrastructure and seasonality

A linear mixed effects modeling approach was used to determine the significant drivers of each gas across streams in different headwater infrastructure categories. Due to uncertainties in the gas flux parameters, GHG saturation ratios were used rather than GHG emissions to compare spatial and temporal patterns across sites. Mixed effects modeling was carried out using R (R Core Team, 2014) and the *nlme* package (Pinheiro et al. 2012) following guidance outlined in Zurr et al. (2009).

Separate mixed effects models were used to detect the role of infrastructure category and date on each response variable. Response variables included saturation ratios for each gas (CO_2, N_2O, and CH_4), solute concentrations (DOC, DIC, TDN, NO_3^-), and organic matter source indices (humification index, autochthonous inputs index). Fixed effects were 'infrastructure category' and 'sampling date,' as well as an interaction term for the two. The effect of a random intercept for 'site' was included in each model.

The statistical assumptions of normality, and equal variances were validated by inspecting model residuals. When necessary, variances were weighted based on infrastructure category to remove heteroscedasticity in model residuals (Zuur et al. 2009). The assumption of temporal independence was examined by testing for temporal autocorrelation in each response variable. This test was performed using the function 'corAR1(),' which is part of the package '*nlme'* in R. to test for temporal autocorrelation. The significance of random effects, weighting variances, and temporal autocorrelation was tested by comparing Akaike information criterion (AIC) scores for models with and without each of these attributes. Additionally, pairwise ANOVA tests were run to determine whether each additional level of model complexity significantly reduced the residual sum of squares. Final model selection was based on meeting model assumptions, minimizing the AIC value, and minimizing residual standard error. Pairwise comparisons among infrastructure categories were examined using the Tukey HSD post-hoc test (*lsmeans* package, Lenth, 2016) for each response variable where 'infrastructure category' had a significant effect. Where 'infrastructure category' did not have a significant effect on a response variable after incorporating 'site' as a random effect, a separate set of linear models was run with 'Site' and 'Date' as main effects rather than 'Infrastructure category'. The role of 'Site' was evaluated in these cases to determine the degree to which site-specific factors overwhelmed the effect of infrastructure category.

Biogeosciences Discuss., doi:10.5194/bg-2016-380, 2016
Manuscript under review for journal Biogeosciences
Published: 15 September 2016

2.4.1 Role of continuous variables on gas saturation

A stepwise linear regression approach was used to examine the role of multiple continuous variables on CO_2, N_2O, and CH_4 saturation across sites and dates. Predictor variables were selected *via* backward stepwise procedure, using the 'Step' function in R. This involves first running a model that includes all potential driving factors, then running sequential iterations of that model after removing one variable at a time until the simplest and most robust combination of predictors was achieved. Model fit at each step was evaluated using the AIC score. Parameters that did not reduce AIC when comparing models were removed until the model had the best fit with the minimum number of factors. The initial list of potential drivers included temperature, DO, DOC, TDN, DIC, humification index (HIX), and the autochthonous inputs index (BIX). Prior to the stepwise regression, we calculated the variance inflation factor (VIF) for each response variable to test for multicolinearity. VIF >3 was the cutoff for assessing multicolinearity. All variables in this study were below the VIF >3 threshold (Zuur et al. 2010).

Analysis of covariance (ANCOVA) was carried out to determine whether relationships among gases (CO_2 vs. N_2O, CO_2 vs. CH_4) and solutes (DOC *vs.* NO_3^-) varied systematically across infrastructure categories. ANCOVA involved comparing two generalized least squares models. The first linear model included an interaction term between one of the predictor variables (i.e. DOC or CO_2) and infrastructure category to predict the response variable (N_2O or CH_4). The second was a linear model with the same two independent variables but no interaction term. When infrastructure category had a significant influence on both the intercept (first model) and slope (second model) of a relationship, this refuted the null hypothesis that infrastructure category had no influence on a relationship.

3 Results

3.1 Effect of urban infrastructure on water quality and DOC:NO_3^- ratios

There were significant differences among TDN, NO_3^-, and DOC: NO_3^- ratios across infrastructure category (Table 2). TDN concentrations ranged from 0.12 to 8.7 mg N L^{-1} (Table 3). Pairwise comparisons yielded significantly higher TDN concentrations in sites in the typology of 'septic systems', compared with the 'in-line SWM wetlands' typology, and sites in the 'riparian/floodplain preservation' typology. Sites in the 'stream burial' typology fell within the mid-range of TDN concentrations and were not different from any other category. DOC concentrations varied widely from 0.19 to 16.89 mg L^{-1}, but were not significantly predicted by infrastructure typology (Table 2). DOC: NO_3^- ratios varied over several orders of magnitude, from 0.02 to 112 (Fig. 2). Infrastructure typology was a significant predictor of DOC: NO_3^-, with the lowest ratios in sites with septic systems and highest in sites with riparian/floodplain preservation (Fig. 2). DOC: NO_3^- ratios did not differ between in the in-line SWM wetland and complete stream burial typologies (Fig. 2)

Biogeosciences Discuss., doi:10.5194/bg-2016-380, 2016
Manuscript under review for journal Biogeosciences
Published: 15 September 2016

3.2 Effects of urban infrastructure on dissolved organic matter quality

Organic matter source metrics, humification index (HIX) and autochthonous inputs index (BIX) showed mixed results. Streams draining septic system infrastructure had significantly lower humification index values than any other infrastructure typology. The autochthonous inputs index (BIX) values showed no significant pattern across infrastructure typologies (Table 2).

3.3 Effects of urban infrastructure on dissolved organic matter quality

Mixed effects models did not detect significant influence of infrastructure typology alone on N_2O, CH_4, and CO_2 saturation in streams. There was, however, a significant interaction effect between sampling date and infrastructure typology on the saturation ratios of all three gases (Table 2). This indicated that sampling date was important to GHG saturation for some infrastructure typologies, or that, the effect of infrastructure may be dependent upon sampling date. The second set of linear models, which used site rather than infrastructure category as a main effect, yielded significant differences across all sites for N_2O (Fig. 3). Similarly, for CO_2, there were significant differences in 25 out of 28 pairwise comparisons. Pairwise comparisons across sites for CH_4 saturation were significant in 23 out of 28 cases. These patterns suggest that site-specific effects overwhelmed the role of infrastructure categories on GHG saturation.

3.4 Effects of urban infrastructure on dissolved organic matter quality

Stepwise model parameter selection yielded several variables that correlate with each GHG saturation ratio (Table 4). TDN was the strongest predictor of N_2O saturation, followed by DO. The final model for N_2O (r^2=0.78) also included temperature, HIX, BIX, %SWM, and DOC:NO_3^-. CO_2 saturation had a similar pattern of predictors and nearly identical model fit (r^2=0.78). DOC:NO_3^- ratio was the strongest predictor of CH_4 saturation followed by DO and temperature. HIX, %IC, and %SWM were also related to CH_4 saturation, but TDN and BIX were not.

3.5 Covariance among GHG abundance and C: N Stoichiometry

N_2O and CH_4 were both correlated with anaerobic CO_2 concentrations, and these relationships varied significantly across infrastructure categories. The relationship between anaerobic CO_2 concentrations and N_2O saturation ratio (Fig. 4a) was more consistent across land use categories than CH_4 saturation ratio *vs.* anaerobic CO_2 (Fig. 4b). There was an overall inverse relationship between NO_3^- and DOC across study sites, but the slope of this relationship differed significantly with land use category (Fig. 4c; ANCOVA p-value < 0.05).

3.6 Longitudinal Patterns in Water, Carbon, Nitrogen, and GHGs

Spatial variability in GHG saturation was examined in order to evaluate whether concentrations measured in tributaries were consistent along the drainage network for Red Run and Dead Run. Very high N_2O saturation ratios were measured in headwaters of both Red Run and Dead Run, which were not representative of the remainder of the drainage network (Fig. 5).

Biogeosciences Discuss., doi:10.5194/bg-2016-380, 2016
Manuscript under review for journal Biogeosciences
Published: 15 September 2016

Instead, a logarithmic decline was observed between the sites with highest N_2O saturation and the main stem along hydrologic flowpaths from engineered headwaters to larger order streams. Headwater CH_4 saturation ratios were not markedly different from that in the main stem.

3.7 Greenhouse gas emissions

Greenhouse gas emissions varied substantially across sites and dates. The magnitude of CO_2, CH_4, and N_2O emissions increased with discharge due to the dependence of K_{20} on slope and velocity. Emissions during three high-flow sampling dates (over 0.015 $m^3 s^{-1}$ for all sites) increased the variance of overall mean gas emission rates estimates. When these high emission rates were removed, average daily CO_2 emissions (± standard error) was twenty to 100-fold higher at DRKV 39.5 (±15.5) g C m^{-2} day^{-1} than the other sites, due in part to the tenfold high stream surface slope at DRKV. Average and standard error of all flux values are listed in Table 5.

4 Discussion

4.1 Overview

This study showed strong relationships between urban water quality and GHG saturation across streams draining different forms of urban infrastructure. N_2O and CO_2 saturation was correlated with nitrogen concentrations, but did not differ between infrastructure typologies. TDN, dissolved oxygen, DOC:NO_3^-, and other GHG predictors did differ among the four infrastructure typologies however, suggesting that infrastructure may have an indirect influence on biogeochemical processes in streams. Relationships between anaerobic CO_2 and N_2O concentrations suggest that anaerobic metabolism contributes to N_2O production along hydrologic flowpaths.

4.2 DOC: Nitrate as a Potential Indicator of Microbial Metabolism

By comparing various forms of infrastructure, results from this study support a growing understanding of the biogeochemical consequences of expanded hydrologic connectivity in urban watersheds. Strong inverse relationships between DOC and NO_3^- were present across all four infrastructure typologies (Fig. 4c), which suggests that organic carbon availability modulates nitrogen loading to streams. DOC availability has been shown to control NO_3^- concentrations across terrestrial and aquatic ecosystems through a variety of coupled microbial processes (Hedin et al. 1998, Kaushal and Lewis 2005, Taylor and Townsend 2010). Varying forms of urban infrastructure also influenced DOC: NO_3^- stoichiometry, which suggests that infrastructure influences C and N inputs and/or microbial metabolism along flowpaths.

Understanding the locations of "hot spots" and the processes responsible for N_2O production and NO_3^- removal in watersheds is useful for informing watershed management. The relationship between N_2O and CO_2 can provide insight into production mechanisms because nitrification consumes CO_2 while denitrification simultaneously produces N_2O and CO_2. We found strong positive relationships between N_2O saturation and anaerobic CO_2 concentrations suggest that denitrification was the source of

Biogeosciences Discuss., doi:10.5194/bg-2016-380, 2016
Manuscript under review for journal Biogeosciences
Published: 15 September 2016

N_2O. By contrast, very low DOC: NO_3^- ratios in stream water with highest N_2O saturation suggest that nitrification was the dominant process at these sites. Taylor and Townsend (2010) suggest that the ideal DOC: NO_3^- stoichiometry for denitrification is 1:1, and that persistent conditions below that are more ideal for nitrification. DOC: NO_3^- was consistently below 1 in streams in septic system infrastructure and consistently above 1 at sites in riparian/floodplain preservation typology, which suggests that DOC and NO_3^- limited in-stream denitrification in these two infrastructure typologies respectively. Conversely, the mean stoichiometric ratio was consistently near 1 in sites with in-line SWM wetlands and stream burial. While DOC: NO_3^- stoichiometry in some streams appeared more favorable for nitrification, the positive anaerobic CO_2 *vs.* N_2O relationships in these streams suggest that these gases were produced anaerobically (by denitrification). One possible explanation for this discrepancy is that the N_2O and CO_2 observed in the stream were produced under stoichiometric conditions more favorable for denitrification along groundwater flow paths prior to emerging in the stream channel. Because sampling took place very close to the origin of the stream network (either buried in pipes or stormwater management wetlands), it is not necessarily surprising that groundwater inputs would dominate the GHG signal.

4.3 Effects of infrastructure on N_2O along the urban watershed continuum

The present study documents some of the highest N_2O concentrations currently reported in the literature for streams and rivers, ranging from 0.009 to 0.55 µM, with a median value of 0.07µM and mean of 0.11 µM N_2O-N. This range of concentration is greater than that reported for headwater agricultural streams in the Midwestern United States (0.03 – 0.07 µM, Werner et al. 2012; 0.03 to 0.15 µM, Beaulieu et al. 2008). A similar range of dissolved N_2O concentrations was reported for macrophyte-rich agriculturally influenced streams in New Zealand (0.06 to 0.60µM, Wilcock and Sorrell, 2008). The only report of higher dissolved N_2O concentrations in streams is from a subtropical stream receiving irrigation runoff, livestock waste, and largely untreated urban sewage (saturation ratio max of 60 compared with 47 in this study; Harrison et al. 2005). Average daily N_2O emission rates ranged from 0.57 to 1.01 mg N_2O-N m^{-2} day^{-1}, excluding the high rates from DRKV, and fell within the range of daily estimates reported for nitrogen enriched agricultural streams in the Midwestern U.S. (mean: 0.84, max: 6.4 mg N_2O-N m^{-2} d^{-1}, Beaulieu et al. 2008) and tropical agricultural streams in Mexico (mean = 0.4, max=5.9 mg N_2O-N m^{-2} d^{-1}, Harrison and Matson 2003). The magnitude of N_2O emissions from urban waterways warrant further study as a potentially significant contributor to global GHG.

N_2O emissions from agricultural runoff are currently included in IPCC estimates, but emissions associated with urban ecosystems are not currently accounted for (Ciais et al. 2013). Urban and agricultural streams are similar in that they receive excess nitrogen inputs from the watershed, including N inputs from contaminated groundwater. Key differences arise when considering N_2O budgets, however. Whereas agricultural stream emissions are estimated based on annual fertilizer inputs, N in urban streams is derived from diffuse, spatially heterogeneous nonpoint sources. For instance, studies in Baltimore have found that atmospheric deposition and human waste contribute approximately 25 % and 50 % of nitrate inputs, while the remainder is derived from soils and plant materials (Kaushal et al. 2011; Pennino et al. 2016). The proportion of these sources and others is likely to vary widely across and within watersheds.

Biogeosciences Discuss., doi:10.5194/bg-2016-380, 2016
Manuscript under review for journal Biogeosciences
Published: 15 September 2016

Recent reviews have suggested that N_2O emissions from human waste (i.e. leaky sewer lines, septic system effluent, dug pits) are important globally but also largely unmeasured (Strokal and Kroeze 2014; UNEP 2013). Direct emissions from wastewater treatment plants (WWTPs) as well as indirect emissions from post-treatment effluent in rivers are currently accounted for in IPCC methodology. However, potential leaks from aging gravity-fed sanitary sewers are not (UNEP 2013). Short et al. (2014) measured N_2O concentrations in WWTP influent from gravity fed sanitary sewers in Australia and determined that gravity fed sanitary sewers are super-saturated with N_2O, with concentrations in excess of equilibrium by as much as 3.5µM. Average daily sewer pipe xsN_2O concentrations were 0.55 µM, which is nearly identical to the maximum xsN_2O measured in the present study (0.54 µM). While wastewater only contributes a portion of excess N in urban streams, further accounting for this source can likely improve urban GHG budgets.

Synoptic surveys of N_2O saturation in Red Run and Dead Run in this study provide evidence that the entire network is a net source of N_2O, despite patterns of 'hot spots' in the headwaters (Fig. 5). Because the headwater sampling sites were located very close to their origin (either in created SWM wetlands or storm drains), it is possible that the highest N_2O concentrations measured represent groundwater-derived GHG production. N_2O saturation declines along the stream network, suggesting that emissions outpace new sources to the water column. The heterogeneous patterns found in gas concentrations both among headwater sites and along the stream network are likely a reflection of variations in dissolved gas and N concentrations in ground water, incomplete denitrification, and differences in groundwater inflow volumes. Detailed information about groundwater inflow patterns and connectivity with N sources along urban stream networks watersheds is a key next step in quantifying as exchange at this scale.

4.4 Effects of infrastructure on CH_4 along the urban watershed continuum

Methane was consistently super-saturated across all streams in this study, and varied significantly across headwater infrastructure categories. The highest CH_4 abundance was measured in sites with riparian reconnection (RRRM and RRRB) followed by streams draining in-line SWM wetlands (DRKV and DRGG) (Fig. 3). As with N_2O and CO_2, CH_4 saturation was negatively correlated with DO, however CH_4 was positively correlated with $DOC:NO_3^-$ while other gases had stronger relationships with TDN (Table 4). These patterns suggest that, along with redox conditions, carbon availability may modulate the relative proportion of different gases that occur in stream water.

Measurements of CH_4 saturation ratio (3.0 to 2157) fell within the lower range of previously measured values in agricultural streams in Canada (sat. ratio 500 to 5000, Baulch et al. 2011a). Mean daily CH_4 emissions estimates in this study (excluding DRKV) varied from 0.2 to 3.5 mg CH_4-C m^{-2} d^{-1} and are an order of magnitude lower than measurements in agricultural streams of New Zealand (Wilcock and Sorrel, 2008; 17-56 mg CH_4-C m^{-2} d^{-1}) and southern Canada (20-172mg C m^{-2} d^{-1}, Baulch et al. 2011). These prior studies also included ebullitive (i.e. bubble) fluxes, whereas the present study only examined diffusive emissions. Wilcock and Sorrel (2008) also measured plant transport where sedge plants with aerenchyma were found. These plant types were not present in this study, although they may be present in adjacent stormwater wetlands and floodplains. The CH_4 emission estimates in the present study have a large margin of uncertainty due to factors related to gas flux parameters

discussed above; however, consistent variations in CH_4 abundance across infrastructure typologies, as well as negative relationships with TDN, suggest that CH_4 is susceptible to human activities such as wetland and floodplain reconnection in urban areas.

Methane concentrations were consistent with prior studies, showing that streams are commonly super-saturated with CH_4 (e.g. Jones and Mulholland 1998; Wilcock and Sorrel 2008; Baulch et al. 2011; Werner et al. 2012). In contrast with IPCC methodology (Ciais et al. 2013), there is growing evidence that human impacts on watersheds influence CH_4 emissions from streams (Kaushal et al. 2014b, Crawford and Stanley 2015; Stanley et al. 2015). Prior studies have found that CH_4 production tends to be elevated in streams with fine benthic sediments, an influx of organic matter, or significant wetland drainage (Dinsmore et al. 2009; Dawson et al. 2002; Baulch et al. 2011). Significant negative relationships between TDN and CH_4 were detected in this study, and elevated CH_4 concentrations in streams draining intact floodplains and/or stormwater management wetlands.

5 Conclusions

Urban watersheds are highly altered systems, with numerous hotspots of biogeochemical activity and GHG emissions. The present study demonstrates that GHG saturation and emissions from urban headwater streams can be similar in magnitude to those of agricultural streams, and warrant further study. Variations in urban infrastructure (i.e. SWM wetlands, riparian connectivity, septic systems) can affect C:N stoichiometry as well as redox state of aquatic ecosystems and significantly alter GHG production. Based on the observed temporal and spatial patterns in this study, variation in nonpoint sources and flowpaths of nitrogen has potential to modify microbial metabolism of organic matter and may contribute significantly to urban GHG budgets.

An increasing number of scientific studies have compiled GHG budgets of anthropogenic and ecological emissions across cities (e.g., Brady and Fath, 2008; Hoornweg et al. 2011; Weissert et al. 2014). Understanding both the anthropogenic and ecological components of a regional GHG budget is crucial for setting GHG targets and managing ecosystem services (Bellucci et al. 2012). The role of human activities on GHG emissions from agriculturally impacted waterways is well recognized (Ciais et al. 2013; Nevison 2000). However, further studies examining the magnitude and variations in GHG emissions along the urban watershed continuum, which explicitly includes flowpaths from engineered infrastructure to streams and rivers (e.g. Kaushal and Belt 2012), are necessary. As cities and populations continue to expand globally, GHG emissions from wastewater are likely to rise. A greater understanding of the interplay between urban water infrastructure and biogeochemical processes is necessary to mitigate negative consequences of N_2O, CH_4, and CO_2.

Code availability: The authors are happy to share any and all codes used to produce this manuscript. Please contact the corresponding author with inquiries about the codes used.

Data availability: The authors have provided tables of all raw data collected for this study in the supplementary information files. These datasets will additionally be available as part of the Baltimore Ecosystem Study LTER Site archive (www.beslter.org).

Author Contributions:

R. Smith, S. Kaushal, C. Welty and M. Pennino selected sampling sites based on infrastructure typology. R. Smith, S. Kaushal and J. Beaulieu designed the gas and solute sampling design. R. Smith and J. Beaulieu analyzed samples for solute and gas concentrations respectively. C. Welty collected continuous flow data from headwater gaging stations. J. Beaulieu provided key insights into interpretation of gas concentrations and statistical analyses and gas flux estimations. M. Pennino provided feedback on multiple versions of the manuscript and data used for estimating K_{20}. S. Kaushal provided funding for the project.

Competing interests: The authors declare that they have no conflict of interest.

Acknowledgements

The authors gratefully acknowledge funding from the National Science Foundation Water Sustainability and Climate program (NSF grants CBET-1058038 and CBET-1058502), as well as scientific infrastructure provided by the Baltimore Ecosystem Study LTER (www.beslter.org, NSF grant DEB-1027188). Field data collection was also partially supported by NOAA grant NA10OAR431220 to the Center for Urban Environmental Research and Education (www.cuere.umbc.edu) and the Water Resources mission area of the U. S. Geological Survey (water.usgs.gov). Daniel Jones provided advice on spatial analyses and numerous individuals including Tamara Newcomer, Tom Doody, Evan McMullen, John Urban, Shahan Haq, Julia Gorman, Julia Miller, John Kemper, Erin Stapleton, and Joshua Cole provided field assistance and/or feedback on drafts of this manuscript. The views expressed in this article are those of the authors and do not necessarily reflect the views or policies of the U.S. Environmental Protection Agency.

References

Aitkenhead-Peterson J.A. and McDowell W.H. : Soil C:N ratio as a predictor of annual riverine DOC flux at local and global scales. Global Biogeochemical Cycles 14:127. doi: 10.1029/1999GB900083, 2000.

Baltimore County Department of Planning. Master Plan 2010, Accessed December 29, 2015; http://resources.baltimorecountymd.gov/Documents/Planning/masterplan/masterplan2010.pdf, 2000.

Bastviken, D., Tranvik, L.J., Downing, J.A.,Crill, P.A., Enrich-Prast, A.: Freshwater methane emissions offset the continental carbon sink. Science Brevia 331:50, 2011.

Baulch, H.M., Dillon, P.J., Maranger, R. and Schiff, S.L.: Diffusive and ebullitive transport of methane and nitrous oxide from streams: Are bubble-mediated fluxes important? Journal of Geophysical Research. doi: 10.1029/2011JG001656, 2011.

Beaulieu, J.J., Arango, C.P., Hamilton, S.K. and Tank, J.L. : The production and emission of nitrous oxide from headwater streams in the Midwestern United States. Global Change Biology 14:878–894. doi: 10.1111/j.1365-2486.2007.01485.x, 2008.

Beaulieu, J.J., Arango, C.P., Tank, J.L.: The effects of season and agriculture on nitrous oxide production in headwater streams. Journal of Environmental Quality 38:637–46. doi: 10.2134/jeq2008.0003, 2009.

Beaulieu, J.J., Shuster, W.D., Rebholz, J.A.: Nitrous oxide emissions from a large, impounded river: the Ohio River. Environmental Science & Technology 44:7527–7533, 2010.

Beaulieu, J.J., Tank, J.L., Hamilton, S.K, Wollheim, W.M., Hall Jr., R.O., Mulholland, P.J., Peterson, B.J., Ashkenas, L.R., Cooper, L.W., Dahm, C.N., Dodds, W.K., Grimm, N.B., Johnson, S.L., McDowell, W.H., Poole, G.C., Valette, H.M., Arango, C.P., Bernot, M.J., Burgin, A.J., Crenshaw, C.L., Helton, A.M., Johnson, L.T., O'Brien, J.M., Potter, J.D., Sheibley, R.W., Sobota, D.J. and Thomas, S.M.: Nitrous oxide emission from denitrification in stream and river networks. Proceedings of the National Academy of Sciences 108:214–219. doi: 10.1073/pnas.1011464108, 2011.

Beaulieu, J.J., Mayer, P.M., Kaushal, S.S., Pennino, M.J., Arango, C.P., Balz, D.A., Canfield, T.J., Elonen, C.M., Fritz, K.M., Hill, B.H., Ryu, H. and Santo Domingo, J.W.: Effects of urban stream burial on organic matter dynamics and reach scale nitrate retention. Biogeochemistry 121:107–126. doi: 10.1007/s10533-014-9971-4, 2014.

Beaulieu, J.J., Golden, H.E., Knightes, C.D., Mayer, P.M., Kaushal, S.S., Pennino, M.J., Arango, C.P., BAlz, D.A., Elonen, C.M., Fritz, K.M. and Hill, B.: Urban Stream Burial Increases Watershed-Scale Nitrate Export. Plos One 10:e0132256. doi: 10.1371/journal.pone.0132256, 2015.

Bellucci, F., Bogner, J.E., Sturchio, N.C.: Greenhouse Gas Emissions at the Urban Scale. Elements 8:445–449. doi: 10.2113/gselements.8.6.445, 2012.

Bhaskar, A.S. and Welty, C.: Water Balances Along an Urban-to-Rural Gradient of Metropolitan Baltimore, 2001–2009, Environ & Engin Geoscience, 18(1), doi:10.2113/gseegeosci.18.1.37, 2012.

Bhaskar, A.S. and Welty, C.: Analysis of subsurface storage and streamflow generation in urban watersheds. Water Resources Research, 51, doi:10.1002/2014WR015607, 2015.

Brady, P.A. and Fath, B.D.: Baltimore County Government Greenhouse Gas Inventory 2002-2006 Projections for 2012. Updated June 18, 2015, Accessed December 31, 2015. http://www.baltimorecountymd.gov/Agencies/environment/sustainability/ghgproject.html, 2008.

Caraco, N.F., Lampman, G., Cole, J.J., Limburg, K.E., Pace, M.L. and Fischer, D.: Microbial assimilation of DIN in a nitrogen rich estuary: Implications for food quality and isotope studies. Marine Ecology Progress Series 167:59–71. doi: 10.3354/meps167059, 1998.

Ciais, P., C. Sabine, G. Bala, L. Bopp, V. Brovkin, J. Canadell, A. Chhabra, R. DeFries, J. Galloway, M. Heimann, C. Jones, C. Le Quéré, R.B. Myneni, S. Piao and P. Thornton.: Carbon and Other Biogeochemical Cycles. In: Climate Change 2013: The Physical Science Basis. Contribution of Working Group I to the Fifth Assessment Report of the Intergovernmental Panel on Climate Change [Stocker, T.F., D. Qin, G.-K. Plattner, M. Tignor, S.K. Allen, J. Boschung, A. Nauels, Y. Xia, V. Bex and P.M. Midgley (eds.)]. Cambridge University Press, Cambridge, United Kingdom and New York, NY, USA, 2013.

Collins, K.A., Lawrence, T.J., Stander, E.K., Jontos, R.J., Kaushal, S.S., Newcomer, T.A., Grimm, N.B. and Cole Ekberg, M.L.: Opportunities and challenges for managing nitrogen in urban stormwater: A review and synthesis. Ecological Engineering 36:1507–1519. doi: 10.1016/j.ecoleng.2010.03.015, 2010.

Crawford, J.T. and Stanley, E.H. Controls on methane concentrations and fluxes in streams draining human-dominated landscapes. Ecological Applications 15–1330.1. doi: 10.1890/15-1330.1, 2015

Dawson, J. J., Billett, M. F., Neal, C. and Hill, S.: A comparison of particulate, dissolved

and gaseous carbon in two contrasting upland streams in the UK, Journal of Hydrology, 257(1–4), 226–246, doi:10.1016/S0022-1694(01)00545-5, 2002.

Dinsmore, K.J., Billett, M.F., Moore, T.R.: Transfer of carbon dioxide and methane through soil-water-atmosphere system at Mer Bleue peatland, Canada. Hydrological Processes 23:330–341. doi: 10.1002/hyp, 2009.

Dodds, W.K., Martí, E., Tank, J.L., Pontius, J., Hamilton, S.K., Grimm, N.B., Bowden, W.B., McDowell, W.H., Peterson, B.J., Valett, H.M., Webster, J.R. and Gregory, S.: Carbon and nitrogen stoichiometry and nitrogen cycling rates in streams. Oecologia 140:458–467. doi: 10.1007/s00442-004-1599-y, 2004

Doheny, E.J.: Index of Hydrologic Characteristics and Data Resources for the Gwynns Falls Watershed. Baltimore County and Baltimore City, Maryland, USGS Open-File Report 99-213, 17 p, 1999.

Doyle, M. W., Stanley, E. H., Havlick, D. G., Kaiser, M. J., Steinbach, G., Graf, W. L., Galloway, G. E. and Riggsbee, J. A.: Aging Infrastructure and Ecosystem Restoration, Science, 319, 286–287, 2008.

Elmore, A.J. and Kaushal, S.S.: Disappearing headwaters: patterns of stream burial due to urbanization. Frontiers in Ecology and the Environment 6:308–312. doi: 10.1890/070101, 2008.

Findlay, S.E.G., McDowell, W.H., Fischer, D., Pace, M.L., Caraco, N., Kaushal, S.S. and Weathers, K.C.: Total carbon analysis may overestimate organic carbon content of fresh waters in the presence of high dissolved inorganic carbon. Limnol Oceanogr Methods 8:196–201, 2010.

Foley, J., de Haas, D., Yuan, Z. and Lant, P.: Nitrous oxide generation in full-scale biological nutrient removal wastewater treatment plants. Water Research 44:831–844. doi: 10.1016/j.watres.2009.10.033, 2010.

Foley, J.A., Defries, R., Asner, G.P., Barford, C., Bonan, G, Carpenter, S.R., Chapin, F.S., Coe, M.T., Daily, G.C., Gibbs, H.K., Helkowski, J.H., Holloway, T., Howard, E.A., Kucharki, C.J., Monfreda, C., Patz, J.A., Prentice, I.C., Ramankutty, N., and Snyder, P.K.: Global consequences of land use. Science 309:570–574. doi: 10.1126/science.1111772, 2005.

Groffman, P.M., Gold, A.J. and Addy, K.: Nitrous oxide production in riparian zones and its importance to national emission inventories. Chemosphere - Global Change Science 2:291–299, 2000.

Groffman, P.M., Law, N.L., Belt, K.T., Band, L.E. and Fisher, G.T.: Nitrogen Fluxes and Retention in Urban Watershed Ecosystems. Ecosystems 7:393–403. doi: 10.1007/s10021-003-0039-x, 2004.

Harrison, J. and Matson, P.A. Patterns and controls of nitrous oxide emissions from waters draining a subtropical agricultural valley. Global Biogeochemical Cycles. doi: 10.1029/2002GB001991, 2003.

Harrison, J.A., Matson, P.A. and Fendorf, S.E.: Effects of a diel oxygen cycle on nitrogen transformations and greenhouse gas emissions in a eutrophied subtropical stream. Aquatic Sciences 67:308–315. doi: 10.1007/s00027-005-0776-3, 2005.

Hedin, L.O., Von Fischer, J.C., Ostrom, N.E., Kennedy, B.P., Brown, M.G. and Robertson, P.G.: Thermodynamic Constraints on Nitrogen Transformations and other Biogeochemical Processes at Soil-Stream Interfaces. Ecological Society of America 79:684–703, 1998.

Hoornweg, D., Sugar, L. and Trejos Gomez, C.L.: Cities and greenhouse gas emissions: moving forward. Environment and Urbanization 23:207–227. doi: 10.1177/0956247810392270, 2011.

Huguet, A., Vacher, L., Relexans, S., Saubusse, S., Froidefond, J.M., Parlanti, E.: Properties of fluorescent dissolved organic matter in the Gironde Estuary. Organic Geochemistry 40:706–719. doi: 10.1016/j.orggeochem.2009.03.002, 2009.

Jones, J.B. and Mulholland, P.J.: Carbon dioxide variation in a Hardwood Forest Stream: An Integrative Measure of Whole Catchment Soil Respiration. Ecosystems 1:183–196, 1998.

Kaushal, S.S. and Lewis, W.M.: Fate and transport of organic nitrogen in minimally disturbed montane streams of Colorado, USA. Biogeochemistry 74:303–321. doi: 10.1007/s10533-004-4723-5, 2005.

Kaushal, S.S., Groffman, P.M., Mayer, P.M., Striz, E. and Gold, A.J.: Effects of stream restoration on denitrification in an urbanizing watershed. Ecological Applications 18:789–804, 2008.

Kaushal, S.S., Groffman, P.M., Band, L.E., Elliott, E.M., Shields, C.A., Kendall, C.: Tracking nonpoint source nitrogen pollution in human-impacted watersheds. Environmental Science & Technology 45:8225–8232, 2011.

Kaushal, S.S. and Belt, K.T.: The urban watershed continuum: evolving spatial and temporal dimensions. Urban Ecosystems 15:409–435. doi: 10.1007/s11252-012-0226-7, 2012.

Kaushal, S.S., Delaney-Newcomb, K., Findlay, S.E., et al: Longitudinal patterns in carbon and nitrogen fluxes and stream metabolism along an urban watershed continuum. Biogeochemistry 121:23–44. doi: 10.1007/s10533-014-9979-9

Kaushal SS, Mayer PM, Vidon PG, et al (2014b) Land use and climate variability amplify carbon, nutrient, and contaminant pulses: A review with management implications. Journal of the American Water Resources Association 50:585–614. doi: 10.1111/jawr.12204, 2014a.

Knowles, R.: "Denitrification." Microbiological Reviews 46: 43-70, 1982.

Lenth, R.V.: Least-Squares Means: The R Package lsmeans. Journal of Statistical Software, 69(1), 1-33, 2016

Mayer, P.M., Groffman, P.M., Striz, E.A. and Kaushal, S.S.: Nitrogen dynamics at the groundwater-surface water interface of a degraded urban stream. Journal of Environmental Quality 39:810–823. doi: 10.2134/jeq2009.0012, 2010.

Meierdiercks, K. L., Smith, J. a., Baeck, M. L. and Miller, A. J.: Analyses of Urban Drainage Network Structure and its Impact on Hydrologic Response, Journal of the American Water Resources Association, 46(5), 932–943, 2010.

Nelson, P.A., Smith, J.A. and Miller, A.J.: Evolution of channel morphology and hydrologic response in an urbanizing drainage basin. Earth Surface Processes and Landforms 31:1063–1079. doi: 10.1002/esp.1308, 2006.

Newcomer, T. A., Kaushal, S. S., Mayer, P. M., Shields, A. R., Canuel, E. A., Groffman, P. M. and Gold, A. J.: Influence of natural and novel organic carbon sources on denitrification in forest, degraded urban, and restored streams. *Ecological Monographs*, *82*(4), 449–466, 2012.

Newcomer Johnson, T.A., Kaushal, S.S., Mayer, P.M. and Grese, M.M.: Effects of stormwater management and stream restoration on watershed nitrogen retention. Biogeochemistry 121:81–106. doi: 10.1007/s10533-014-9999-5, 2014.

Nevison, C.: Review of the IPCC methodology for estimating nitrous oxide emissions associated with agricultural leaching and runoff. Chemosphere - Global Change Science 2:493–500. doi: 10.1016/S1465-9972(00)00013-1, 2000.

Ohno, T.: Fluorescence inner-filtering correction for determining the humification index of dissolved organic matter. Environmental Science & Technology 36:742–746, 2002.

Pennino, M.J., Kaushal, S.S., Beaulieu, J.J., Mayer, P.M., and Arango, C.P.: Effects of urban stream burial on nitrogen uptake and ecosystem metabolism: implications for watershed nitrogen and carbon fluxes. Biogeochemistry 121:247–269. doi: 10.1007/s10533-014-9958-1, 2014.

Pennino, M.J., Kaushal, S.S., Mayer P.M., Utz, R.M., and Cooper, C.A.: Stream restoration and sanitary infrastructure alter sources and fluxes of water, carbon, and nutrients in urban watersheds. Hydrol. Earth Syst. Sci. 20: 3419-3439. doi: 10.5194/hess-20-3419-2016, 2016.

Pinheiro, J., Bates, D., DebRoy, S. and Sarkar, D: nlme: Linear and nonlinear mixed effects models, 2012.

Raymond, P.A., Hartmann, J., Lauerwald, R., Sobek, S., McDonald, C., Hoover, M., Butman, D., Striegl, R., Mayorga, E., Humborg, C., Kortelainen, P., Dürr, H., Meybeck, M., Ciais, P. and Guth, P.: Global carbon dioxide emissions from inland waters. Nature 503:355–359. doi: 10.1038/nature12760, 2013.

Richey, J.E., Devol, A.H., Wofsy, S.C., Victoria, R., and Ribiero, M.N.G.: Biogenic Gases and the Oxidation and Reduction of Carbon in Amazon River and Floodplain Waters. Limnology and Oceanography 33:551–561, 1988.

Rosamond, M.S., Thuss, S.J. and Schiff, S.L.: Dependence of riverine nitrous oxide emissions on dissolved oxygen levels. Nature Geoscience 5:715–718. doi: 10.1038/ngeo1556, 2012.

Ryan, R.J., Welty, C. and Larson, P.C.: Variation in surface water-groundwater exchange in an urban stream. Journal of Hydrology, 392 (2010) 1–11. doi:10.1016/j.jhydrol.2010.06.004, 2010.

Schlesinger, W. H.: Biogeochemistry: An Analysis of Global Change (Second). New York: Academic Press, 1997.

Seitzinger, S.P., Kroeze, C., Styles, R.V.: Global distribution of N_2O emissions from aquatic systems: Natural emissions and anthropogenic effects. Chemosphere - Global Change Science 2:267–279. doi: 10.1016/S1465-9972(00)00015-5, 2000.

Stumm, W. and Morgan, J. J.: Aquatic chemistry: An introduction emphasizing chemical equilibria in natural waters. New York: John Wiley, 1981.

Shields, C.A., Band, L.E., Law, N., Groffman, P.M., Kaushal, S.S., Savvs, K., Fisher, G.T., and Belt, K.T.: Streamflow distribution of non–point source nitrogen export from urban-rural catchments in the Chesapeake Bay watershed. Water Resources Research 44:1–13. doi: 10.1029/2007WR006360, 2008.

Short, M.D., Daikeler, A., Peters, G.M., Mann, K., Ashbolt, N.J., Stuetz, R.M., and Peirson, W.L.: Municipal gravity sewers: An unrecognized source of nitrous oxide. Science of the Total Environment 468-469:211–218. doi: 10.1016/j.scitotenv.2013.08.051, 2014.

Sivirichi, G.M., Kaushal, S.S., Mayer, P.M., Welty, C., Belt, K.T., Newcomer, T.A., Newcomb, K.D., and Grese, M.M.: Longitudinal variability in streamwater chemistry and carbon and nitrogen fluxes in restored and degraded urban stream networks. Journal of Environmental Management 13:288–303. doi: 10.1039/c0em00055h, 2011.

Smith, R.M. and Kaushal, S.S.: Carbon cycle of an urban watershed: exports, sources, and metabolism. Biogeochemistry. doi: 10.1007/s10533-015-0151-y, 2015.

Søvik, A.K., Augustin, J., Heikkinen, K., Huttunen, J.T., Necki, J.M., Karjalainen, S.M., Kløve, B, Liikanen, A., Mander, Ü., Puustinen, M., Teiter, S., and Wachniew, P.: Emission of the greenhouse gases nitrous oxide and methane from constructed wetlands in Europe. Journal of environmental quality 35:2360–73. doi: 10.2134/jeq2006.0038, 2006.

Stanley, E.H., Casson, N.J., Christel, S.T., Crawford, J.T., Loken, L.C., and Oliver, S.K.: The ecology of methane in streams and rivers: patterns, controls, and global significance. Ecological Monographs 1689–1699. doi: doi: 10.1890/15-1027.1, 2015.

Strokal, M. and Kroeze, C.: Nitrous oxide (N2O) emissions from human waste in 1970–2050. Current Opinion in Environmental Sustainability 9-10:108–121. doi: 10.1016/j.cosust.2014.09.008, 2014.

Taylor, P.G. and Townsend, A.R. Stoichiometric control of organic carbon-nitrate relationships from soils to the sea. Nature 464:1178–1181. doi: 10.1038/nature08985, 2010.

Townsend-Small, A., Pataki, D.E., Czimczik, C.I. and Tyler, S.C.: Nitrous oxide emissions and isotopic composition in urban and agricultural systems in southern California. Journal of Geophysical Research 116:G01013. doi: 10.1029/2010JG001494, 2011.

Tsivoglou, E.C. and Neal, L.A.: Tracer measurement of reaeration: III. Predicting the reaeration capacity of inland streams. Journal (Water Pollution Control Federation) 48:2669–2689, 1976.

R Core Team: R: a language and environment for statistical computing, 2014.

UNEP (United Nations Environment Programme): Drawing Down N_2O To Protect Climate and the Ozone Layer, 2013.

VanderZaag, A.C., Gordon, R.J., Burton, D.L., Jamieson, R.C., and Stratton, G.W.: Greenhouse gas emissions from surface flow and subsurface flow constructed wetlands treating dairy wastewater. Journal of environmental quality 39:460–71. doi: 10.2134/jeq2009.0166, 2010.

Weiss, R. F.: Carbon Dioxide in Water and Seawater: The Solubility of a Non-Ideal Gas, Marine Chemistry, 2, 203–215, 1974.

Weissert, L.F., Salmond, J.A. and Schwendenmann, L.: A review of the current progress in quantifying the potential of urban forests to mitigate urban CO_2 emissions. Urban Climate 8:100–125. doi: 10.1016/j.uclim.2014.01.002, 2014.

Werner, S.F., van Kessel, C., Browne, B.A. and Driscoll, C.T.: Three-dimensional spatial patterns of trace gas concentrations in baseflow-dominated agricultural streams: implications for surface–ground water interactions and biogeochemistry. Biogeochemistry 107:319–338. doi: 10.1007/s10533-010-9555-x, 2012.

Wilcock, R.J. and Sorrell, B.K.: Emissions of Greenhouse Gases CH_4 and N_2O from Low-gradient Streams in Agriculturally Developed Catchments. Water, Air, and Soil Pollution 188:155–170. doi: 10.1007/s11270-007-9532-8, 2008.

Wymore, A.S., Rodríguez-Cardona, B., McDowell, W.H.: Direct response of dissolved organic nitrogen to nitrate availability in headwater streams. Biogeochemistry 126:1–10. doi: 10.1007/s10533-015-0153-9, 2015.

Yamamoto, S., Alcauskas, J. B. and Crozier, T. E.: Solubility of methane in distilled water and sea water, Journal of Chemical and Engineering Data, 21(1), 78–80, doi:10.1021/je60068a029, 1976.

Yu, Z., Deng, H., Wang, D., Ye, M., Tan, Y., Li, Y., Chen, Z., and Xu, S.: Nitrous oxide emissions in the Shanghai river network: Implications for the effects of urban sewage and IPCC methodology. Global Change Biology 19:2999–3010. doi: 10.1111/gcb.12290, 2013.

Zsolnay, A., Baigar, E., Jimenez, M., Steinweg, B., and Saccomandi, F.: Differentiating with fluorescence spectroscopy the sources of dissolved organic matter in soils subjected to drying. Chemosphere 38:45–50, 1999.

Zuur, A., Ieno, E.N., Walker, N., Savilev, A.A., and Smith, G.M.: Mixed Effects Models and Extensions in Ecology with R. doi: 10.1007/978-0-387-87458-6, 2009.

Zuur, A., Ieno, E.N. and Elphick, C.S.: A protocol for data exploration to avoid common statistical problems. A protocol for data exploration to avoid common statistical problems 1:3–14, 2010.

Biogeosciences Discuss., doi:10.5194/bg-2016-380, 2016
Manuscript under review for journal Biogeosciences
Published: 15 September 2016

Tables

Table 1. Summary of site characteristics including drainage area (km^2), percent impervious cover, and percent of the watershed drained by green infrastructure (GI) (i.e. stormwater wetlands).

Typology based on dominant infrastructure feature	Site	Drainage area (km^2)	Percent impervious surface cover	% of land draining GI SWM systems	Description
Septic Systems	RRSD	0.23	7.9	0.00	Low-density residential development with septic systems, minimal GI with some stream burial.
	RRSM	0.68	3.78	13.97	
Floodplain Preservation	RRRM	0.63	16.4	100.00	Suburban and commercial low-impact development converted from agriculture in early 2000s. Stormwater wetlands in upland + wide riparian buffer zones surround each stream and sanitary sewer infrastructure.
	RRRB	0.21	22.81	54.67	
In-line SWM Wetlands	DRKV	0.31	39.16	100.00	Older suburban development (circa 1950s) with GI located in-line with stream channels, rather than dispersed across the landscape. Entire watershed is serviced by sanitary sewers.
	DRGG	0.6	36.68	47.60	
Stream Burial	DRAL	0.26	41.9	1.10	Suburban and commercial development circa 1950s with piped headwaters upstream of the sampling point. Entire watershed is serviced by stormwater pipes and sanitary sewers. No GI present.
	DRIS	0.18	30.57	0.00	

Biogeosciences Discuss., doi:10.5194/bg-2016-380, 2016
Manuscript under review for journal Biogeosciences
Published: 15 September 2016

Table 2 Summary of results (main effects p-values) from mixed effects models examining the role of infrastructure typology and date on each response variable (CO_2, N_2O and CH_4 saturation ratios; TDN and DOC concentrations mg L^{-1}, autochthonous productivity index (BIX) and humification index (HIX)).

Main Effects	CO_2	N_2O	CH_4	TDN	DOC	BIX	HIX	DOC: NO_3^-
Infrastructure typology p-value	0.496	0.488	0.298	0.068	0.200	0.441	0.020	<0.001
Date p-value	0.957	<0.01	0.001	0.086	0.387	0.155	0.765	0.492
Date by Infrastructure Typology Interaction p-value	<0.01	<0.01	0.000	0.114	0.978	0.490	0.899	0.894

Biogeosciences Discuss., doi:10.5194/bg-2016-380, 2016
Manuscript under review for journal Biogeosciences
Published: 15 September 2016

Table 3. Mean with standard error in parentheses of GHG saturation ratios, TDN and DOC concentrations (mg L^{-1}), autochthonous productivity index (BIX) values and humification index (HIX) values for each site.

Infrastructure Typology	Site	CO_2	N_2O	CH_4	TDN	DOC	BIX	HIX	DOC: NO_3^-
Septic Systems	RRSD	52.9 (1.1)	28.0 (0.7)	14.9 (0.5)	6.40 (0.20)	0.76 (0.12)	0.89 (0.02)	0.74 (0.01)	0.06 (0.01)
	RRSM	13.5 (0.5)	5.9 (0.2)	25.6 (1.5)	3.49 (0.13)	1.40 (0.25)	0.70 (0.02)	0.782 (0.015)	0.27 (0.04)
Floodplain Preservation	RRRM	6.6 (0.3)	1.7 (0.04)	207.3 (36.2)	0.59 (0.08)	2.89 (0.27)	0.67 (0.01)	0.85 (0.02)	12.16 (3.45)
	RRRB	9.6 (0.4)	3.6 (0.1)	103.6 (8.6)	0.35 (0.02)	1.58 (0.18)	0.716 (0.01)	0.85 (0.01)	9.24 (2.43)
In-line SWM	DRKV	28.1 (1.0)	19.1 (0.6)	50.8 (8.5)	2.52 (0.16)	2.65 (0.24)	0.75 (0.01)	0.86 (0.003)	2.38 (0.67)
	DRGG	16.3 (1.1)	7.9 (0.4)	225.8 (31.9)	1.16 (0.07)	5.32 (0.60)	0.73 (0.02)	0.83 (0.01)	8.72 (2.23)
Stream Burial	DRAL	7.9 (0.3)	5.1 (0.2)	11.3 (0.6)	2.68 (0.09)	2.64 (0.37)	0.81 (0.01)	0.83 (0.01)	1.42 (0.40)
	DRIS	22.6 (1.0)	10.7 (0.5)	78.4 (5.8)	2.42 (0.09)	2.51 (0.27)	0.79 (0.01)	0.82 (0.01)	1.82 (0.44)

Biogeosciences Discuss., doi:10.5194/bg-2016-380, 2016
Manuscript under review for journal Biogeosciences
Published: 15 September 2016

Table 4. Main effects, model coefficients, adjusted r^2, and overall model p-value for stepwise regression models examining the relationship between continuous variables and GHG saturation ratios. The model coefficient is the main effect of each parameter, and the absolute value of this coefficient signifies the relative contribution of each predictor. * Indicate the predictor with the greatest influence for each response variable (CO_2, N_2O and CH_4). 'n.a.' indicates that the predictor variable was not retained in the final model.

	CO_2	N_2O	CH_4
Predictor	Coefficient	Coefficient	Coefficient
TDN	1.08*	1.10*	n.a.
Temperature	-0.22	-0.26	0.25
DO	-0.46	-0.37	-0.27
HIX	0.09	0.13	-0.15
BIX	0.11	0.15	n.a.
%IC	n.a.	0.14	-0.16
%SWM	0.18	0.31	0.16
log(DOC:NO_3^-)	0.32	0.19	0.55*
Overall Model Fit			
Adjusted r^2	0.78	0.78	0.5
P-value	<0.0001	<0.0001	<0.0001

Biogeosciences Discuss., doi:10.5194/bg-2016-380, 2016
Manuscript under review for journal Biogeosciences
Published: 15 September 2016

Table 5. Summary of gas flux estimations for the four sites with continuous flow data. Average, standard error (s.e.), and number of measurements (n) are listed for CO_2 (g C m^{-2} day^{-1}), CH_4 (mg C m^{-2} day^{-}) and N_2O (mg N m^{-2} day^{-}) as well as predicted K_{20} normalized to O_2.

Infrastructure typology	Site	Gas	Average	s.e.	n
Stream Burial	DRAL	CO_2	0.50	0.18	17
In-line SWM	DRGG		0.64	0.10	15
In-line SWM	DRKV		39.55	8.72	19
Floodplain Preservation	RRRB		2.04	0.48	17
Stream Burial	DRAL	CH_4	0.18	0.09	17
In-line SWM	DRGG		1.53	0.35	15
In-line SWM	DRKV		29.41	21.69	19
Floodplain Preservation	RRRB		3.53	1.13	17
Stream Burial	DRAL	N_2O	0.57	0.22	17
In-line SWM	DRGG		0.53	0.09	15
In-line SWM	DRKV		44.07	9.79	19
Floodplain Preservation	RRRB		1.01	0.23	17
Stream Burial	DRAL	K_{20}	2.29	0.75	17
In-line SWM	DRGG		1.67	0.33	15
In-line SWM	DRKV		57.56	9.63	19
Floodplain Preservation	RRRB		9.36	1.67	17

5

Biogeosciences Discuss., doi:10.5194/bg-2016-380, 2016
Manuscript under review for journal Biogeosciences
Published: 15 September 2016

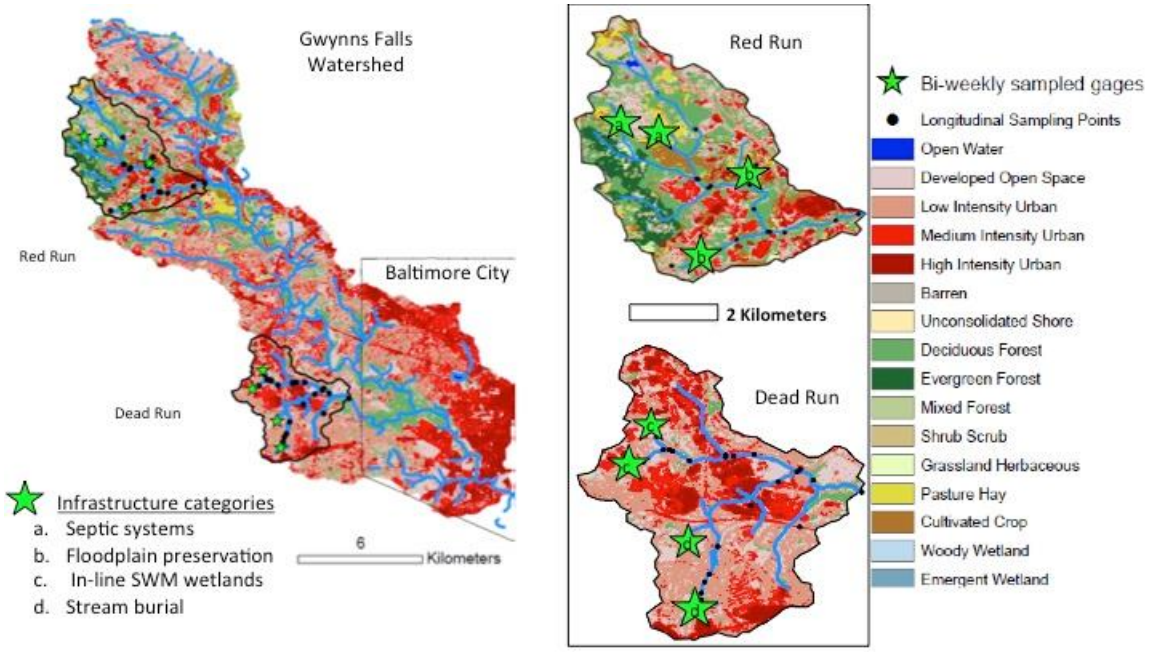

Figure 1: Site map of headwater stream sites within Red Run and Dead Run watersheds. Green stars signify bi-weekly sampling sites and black dots signify longitudinal sampling points sampled seasonally. Land cover categories are colored based on the National Land Cover Database, with dark red areas signifying dense urban land cover, light red signifying medium urban land cover, and green colors signifying forested or undeveloped areas. Close-up views of Dead Run and Red Run on the right represent the study watersheds, with areas that are captured by stormwater management structures (detention basins, wetlands, sand filters, etc.) shaded in gray.

Biogeosciences Discuss., doi:10.5194/bg-2016-380, 2016
Manuscript under review for journal Biogeosciences
Published: 15 September 2016

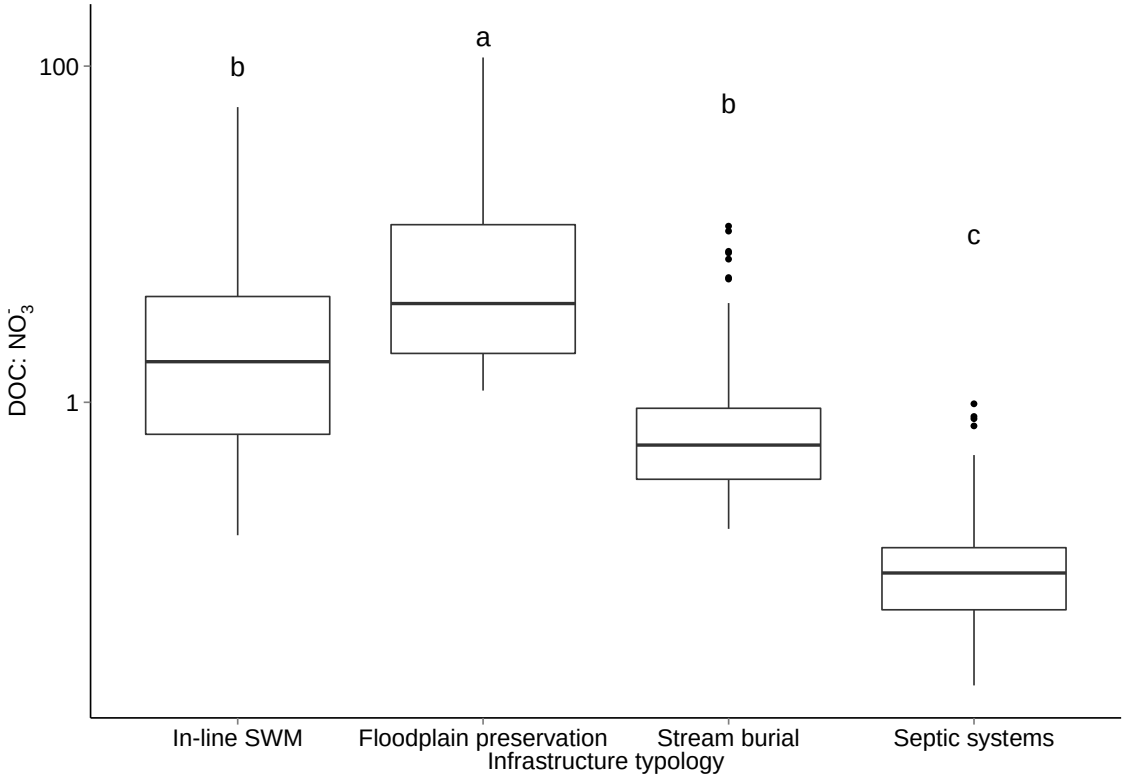

Figure 2 Boxplot of molar DOC: NO_3^- ratio across sites in watersheds with differing infrastructure typologies. The median of each dataset is signified by the middle horizontal line for each category. Boxes signify the range between first and third quartiles (25th and 75th percentiles). Vertical lines extend to the minimum and maximum points in the dataset that are within 1.5 times the inter-quartile range. Points signify data points that fall above or below this range. Letters represent significant ($p < 0.01$) differences between infrastructure typologies for DOC:NO_3^- across all sampling dates, determined using a linear mixed effects model.

Biogeosciences Discuss., doi:10.5194/bg-2016-380, 2016
Manuscript under review for journal Biogeosciences
Published: 15 September 2016

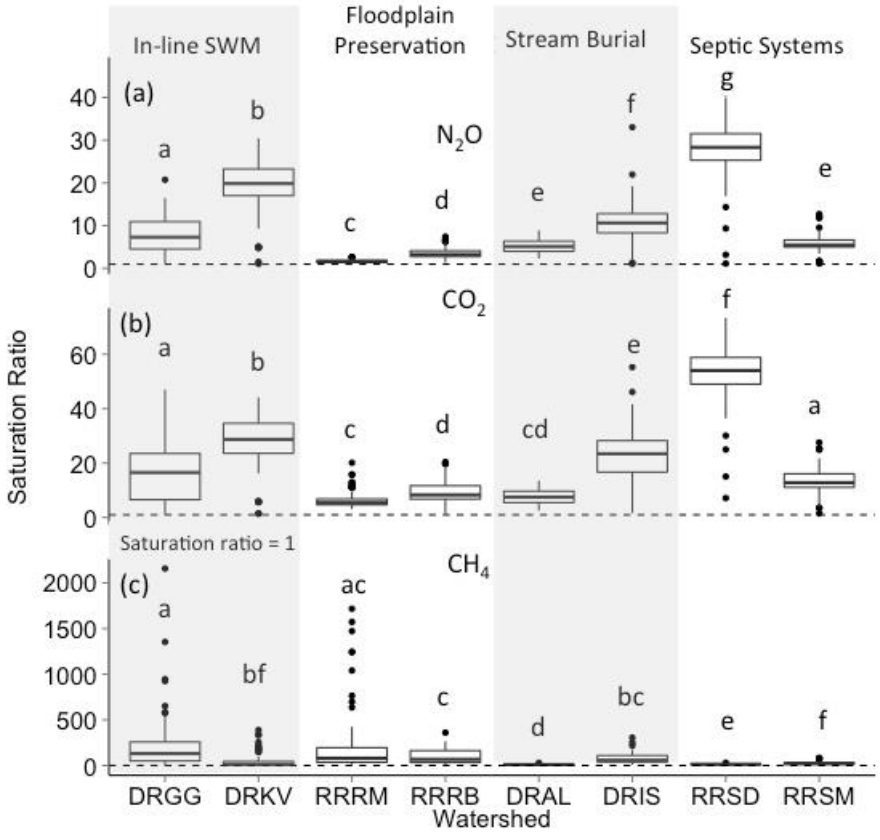

Figure 3 Boxplot of CO_2, CH_4, and N_2O saturation ratios across stream sites in varying infrastructure categories. Letters denote significant pairwise differences across streams for a given gas from linear mixed effects models with 'watershed' as a main effect. Box and whiskers signify the median, first and third quartiles, and points signify outliers outside of 1.5 times the interquartile range.

Biogeosciences Discuss., doi:10.5194/bg-2016-380, 2016
Manuscript under review for journal Biogeosciences
Published: 15 September 2016

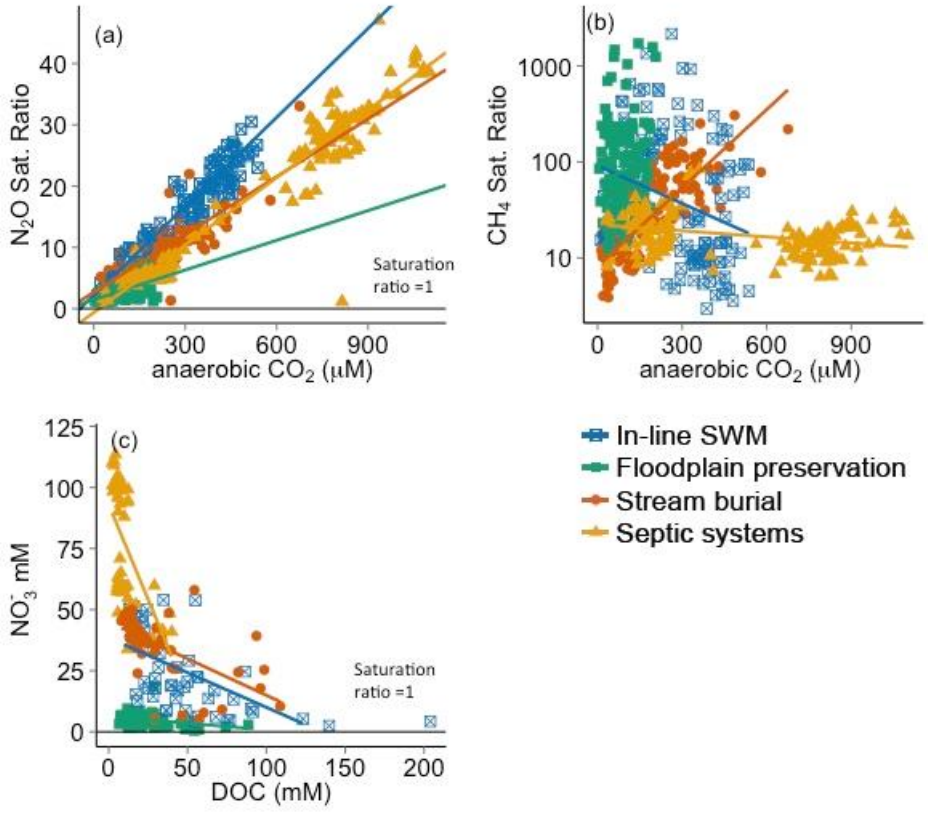

Figure 4. Scatterplots of a) N_2O saturation *vs.* anaerobic CO_2, CH_4 saturation *vs.* anaerobic CO_2, and c) relationships between NO_3^- and DOC. Lines denote significant ($p<0.01$) correlations among gas or solute concentrations, which vary by infrastructure category.

Biogeosciences Discuss., doi:10.5194/bg-2016-380, 2016
Manuscript under review for journal Biogeosciences
Published: 15 September 2016

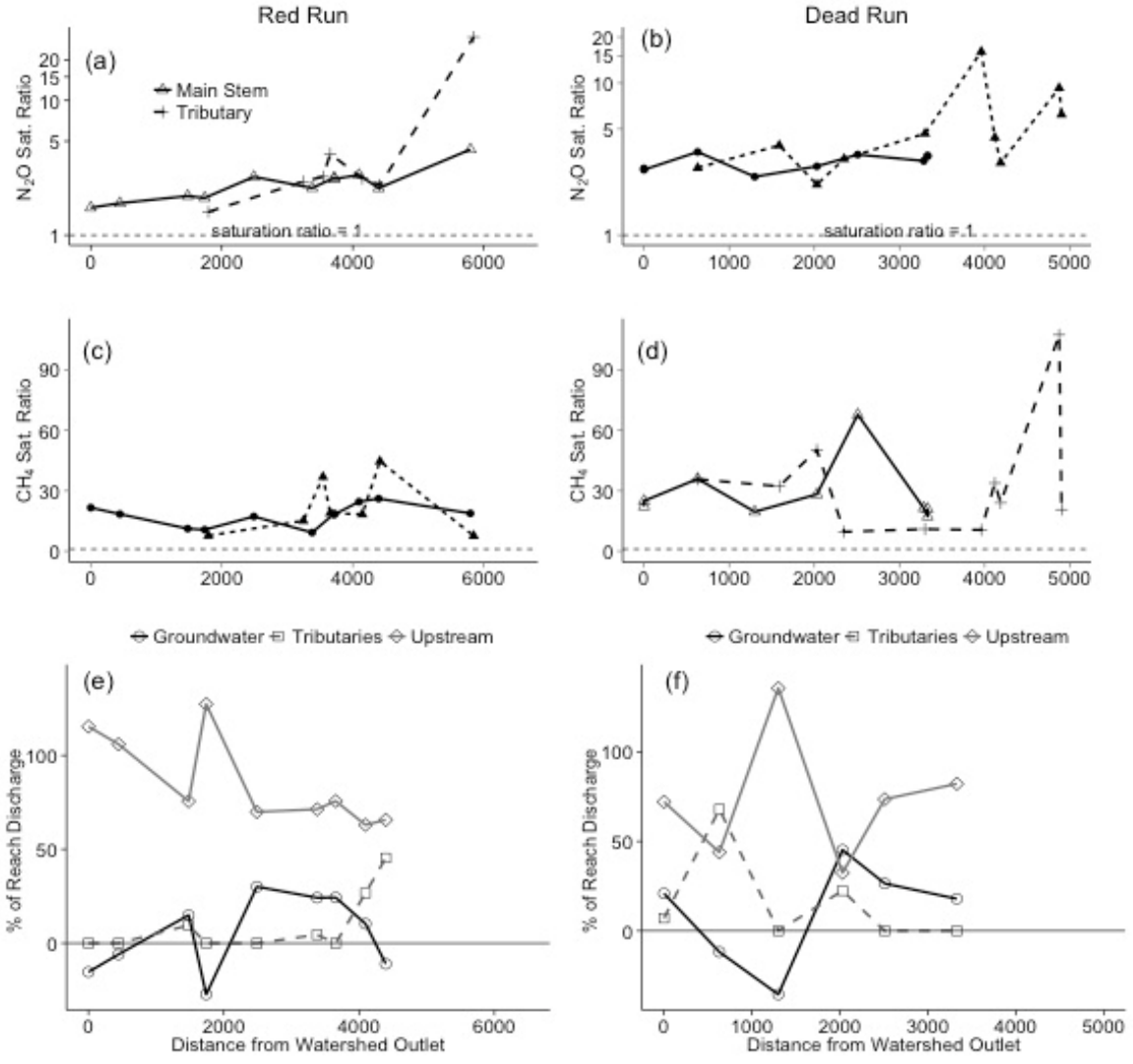

Figure 5. Panels A:D show longitudinal variability in CO_2, N_2O, and CH_4 saturation ratios from a spring synoptic survey in Red Run (left panels) and Dead Run (right panels). The horizontal dashed line in panels a through d signify a saturation ratio of 1. Panels e through f display the proportion of discharge at each sampling location from tributaries, surface water upstream of the reach, and groundwater inflow along the main stem reaches. Negative values for groundwater signify losing reaches of the stream.